INTERNATIONAL JOURNAL OF CLIMATOLOGY
Int. J. Climatol. (2008)
Published online in Wiley InterScience
(www.interscience.wiley.com) DOI: 10.1002/joc.1659

RMetS
ROYAL METEOROLOGICAL SOCIETY

Global summer monsoon rainy seasons

Suping Zhang[a]* and Bin Wang[a,b]

[a] *Physical Oceanography Laboratory and Ocean – Atmosphere Interaction and Climate Laboratory, Ocean University of China, Qingdao, China*
[b] *Department of Meteorology and International Pacific Research Institute, School of Ocean and Earth Science and Technology, University of Hawaii, Hawaii*

ABSTRACT: A concise and objective definition of monsoon rainy season characteristics is proposed for worldwide monsoon regions. The result highlights six major summer monsoon rainy season domains and the mean dates of the local onset, peak and withdrawal phases of the summer monsoon rainy season. The onset phases occur progressively later poleward in the continental domains but primarily eastward in the oceanic monsoon regions. The rainy season retreats equatorward over the continental and oceanic monsoon regions. The length of the rainy season decreases poleward and shorter rainy season can also be found over the outskirts of warm water. Some exceptions exist in terms of the characteristics of rainy season, e.g. the westward advance of rainy season over North Africa and an apparently prolonged rainy season in the Korean peninsula. The results here are basically compatible with those obtained in previous studies on regional monsoons.

A definition of the seasonal wind overturning is proposed. Combining rainfall and winds, we stratify the global monsoon into strong and weak categories. The strong monsoons are typically in the regions with both concentration of summer rainfall and annual reversal of low-level winds, while the weak monsoon features only a contrasting wet–dry season. Seemingly, some mid-latitude regions with wind reversals are not monsoonal because of the reversals being opposite to the monsoon overturning and the rainfall patterns being more or less Mediterranean.

The comparison between the monsoon domains derived from Climate Prediction Center (CPC) Merged Analysis of Precipitation (CMAP) and the 40-year European Centre for Medium-Range Weather Forecasts Re-Analysis (ERA-40), the Japanese 25-year Reanalysis (JRA-25) and National Centers for Environmental Prediction (NCEP) datasets show good capabilities of the reanalyses in demarcation of the major monsoon rainy season domains in the tropics and subtropics. But the reanalyses are less realistic in the mid-latitudes of Eurasia and North America. The result here provides the simple yet objective definitions of monsoon domain, onset, peak and withdrawal which are useful for validation of GCMs. Copyright © 2008 Royal Meteorological Society

KEY WORDS global monsoon rainy season; domain; onset; withdrawal

Received 22 July 2006; Revised 8 October 2007; Accepted 31 October 2007

1. Introduction

Monsoon covers both oceans and continents. The term 'monsoon' originally stems from the Arabic word 'mausim', meaning seasonal prevailing winds (www.metoffice.gov.uk). That is why early studies dealt with monsoon in terms of wind frequency (e.g. Ramage, 1971). Nowadays, monsoon is more generally applied to tropical and subtropical seasonal reversals in both the atmospheric circulation and associated precipitation (Trenberth *et al*., 2000; Trenberth *et al*., 2006). People are more concerned about the precipitation not only because natural disasters like flooding and drought that affect the planting, harvesting, economy and casualty of life are tightly linked to monsoon rainfall, but also because the huge amount of latent heat released in the process of precipitation plays an important part in the global diabatic heating. In fact, monsoon distribution indicates the location of the atmospheric heat source that drives tropical circulation; and thus, rainfall variation reflects the variability of the entire monsoon circulation system (Wang and Ding, 2006).

Monsoon arises from the annual reversals in heating and temperature gradients between continental regions and the adjacent oceans with the progression of the seasons (Trenberth *et al*., 2006). Trenberth and his collaborators have depicted the seasonal variations of the precipitation–evaporation and the associated transport of the latent energy. They pointed out the importance of treating monsoon in a global perspective from the conservation of water and energy (Trenberth *et al*., 2000; Trenberth *et al*., 2006). Wang and Ding (2006) further defined the global monsoon summer rainy season domain in terms of objective thresholds depicting the strength and seasonal distribution of precipitation. They also proposed a metrics to measure the variability of the global monsoon strength and found that in the last 25 years, the global continental monsoon precipitation has been

* Correspondence to: Suping Zhang, Physical Oceanography Laboratory and Ocean – Atmosphere Interaction and Climate Laboratory, Ocean University of China, Qingdao, PRC. 266003, China.
E-mail: zsping@ouc.edu.cn

levelled off whereas the oceanic monsoon precipitation has strengthened.

So far, majorities of the literatures on monsoon rainfall climatological characteristics have been confined to regional monsoons, such as the Indian monsoon (e.g. Rao, 1976; Lau and Yang, 1997), the East Asian monsoon (e.g. Chen *et al*., 1991), the Indonesian and Australian monsoon (e.g. Wang *et al*., 2003; Wheeler and McBride, 2005), the South African monsoon (e.g. Cook, 2000), the South American monsoon (e.g. Rao *et al*., 1996; Charles *et al*., 2002), the West African monsoon (e.g. Grodsky and Carton, 2001; Sultan and Janicot, 2003a) and the North American monsoon (e.g. Adams and Comrie, 1997; Anderson *et al*., 2000). Wang and LinHo (2002) proposed a set of simple objective criteria to describe the Asian summer monsoon (ASM) rainy seasonal characteristic and link the continental monsoon with the adjacent oceanic monsoon regions. While Wang (1994) delineated the global tropical monsoon regimes by outgoing longwave radiation (OLR) and highly reflective clouds (HRC), our knowledge on global monsoon rainy season characteristics has long been falling short due to lack of long-term reliable data, especially the observations over the monsoon ocean regions.

Because it has not been possible, in the past, to obtain a reliable precipitation over the ocean, a variety of proxy variables and ways have been used to define monsoon domain as well as its onset, peak and withdrawal phases, thus, leading to different results. The discrepancies are already significant when we merely talk about the Asian monsoon as discussed in detail in Wang and LinHo (2002). So, it is necessary to develop a universal definition of monsoon and criteria for quantitative description of rainfall climatology in the entire global monsoon regime.

One of the objectives of this study is to extend the work of Wang and LinHo (2002) to investigate the feasibility of using a concise yet pertinent rainfall parameter and a set of universal criteria to quantify rainy season characteristics for all monsoon regions worldwide. Another purpose is to use the precipitation data derived from satellite observations over the oceans along with rain gauge observations over the continent to build up a unified picture of the spatial and temporal structures of the mean monsoon rainy seasons. Efforts are made on the perspectives of the global monsoon regimes combining the annual variations in winds and precipitation. A contrast between different datasets in the delineation of summer monsoon domains is made. The results will provide an observational basis for validation and identification of the possible weaknesses of the existing atmospheric general circulation models and the climate system models in simulating the global summer monsoons.

In Section 2, we describe the dataset and the processing procedure. In Section 3, an innovative and succinct rainfall parameter is proposed to define objectively the rainy season domain. Section 4 presents the resultant onset, peak and withdrawal patterns of the global monsoon rainy season. In Section 5, combining the reversals in winds, we elaborate on the global summer monsoon regimes. And the results derived from different datasets are compared. The last section summarizes our conclusions.

2. Data

The primary datasets analysed in this study include the Climate Prediction Center (CPC) Merged Analysis of Precipitation (CMAP) (Xie and Arkin, 1997), reanalysis data from the National Centers for Environmental Prediction–National Center for Atmospheric Research (NCEP–NCAR) (Kalnay *et al*., 1996), the 40-year European Centre for Medium-Range Weather Forecasts reanalysis (ERA-40) (Simmons and Gibson, 2000) and the Japanese 25-year reanalysis (JRA-25) (Sakamoto *et al*., 2007) monthly mean data. The CMAP is derived by merging rain gauge observations, five satellite estimates and numerical model outputs. The CMAP climatological pentad (5-day) mean (CPM) and monthly mean precipitation rate values are constructed from 1979 to 2004 with global coverage 88.75 °N to 88.75 °S and 1.25 °E to 358.75 °E (eastward) on 2.5 × 2.5 grids. The NCEP and ERA-40 monthly mean data covers the same grid points 144 × 73 on 2.5 × 2.5 geographical degrees, and the JRA-25 are gridded by 320 × 160.

Over the ocean, the accuracy and reliability of the pentad mean CMAP on small spatial scales has not been fully determined because of the lack of ground truth observations. Since the CMAP dataset merges multi-source estimates, the uncertainties contained in each individual estimate are significantly reduced. A comparative study of CMAP and land-based rain gauge data shows that the two datasets yield similar large-scale pictures over land areas (Wang and LinHo, 2002). Thus, it is meaningful to describe large-scale rainfall characteristics using CMAP.

The reconstructed climatological pentad mean (RCPM) rainfall time series resulting from Fourier truncation with the sum of the first 12 harmonics (period longer than 1 month), and consisting of both the seasonal and subseasonal signals and removing the sub-monthly vibration, is best suited for our purpose. In the following analysis of rainfall, we will use the reconstructed pentad rainfall data series to define the onset, peak and withdrawal of the monsoon rainy season. The RCPM precipitation consists of a smoothed annual cycle and a climatological intraseasonal oscillation (CISO). The CISO component is included because it represents sub-seasonal variation, an intrinsic component of the monsoon climate (Lin and Wang, 2002). Wang and Xu (1997) have shown the statistical significance of the CISO in the boreal summer monsoon domain by using a sign test, an extreme test (Monte Carlo simulations) and an amplitude test (the *t*-test).

3. Domains of summer monsoon rainy season

3.1. EOF (empirical orthogonal function) analysis

The annual cycle is usually divided into four seasons: spring, summer, autumn and winter, and each season

DOI: 10.1002/joc

consists of three months. In China, the 24 Solar Terms which mean that the annual cycle is divided into 24 jieqi (periods) based on seasonal variations and agricultural activities, e.g. spring begins, the rains, insects awaken, vernal equinox, clear and bright, grain rain, summer begins, grain buds, grain in ear, summer solstice and etc. have long been used to depict the annual cycle since the ancient time. Summer monsoon may start as early as in May in the South China Sea (SCS) and as late as in July in North China (Tao and Chen, 1987). In this study, we use EOF method to extract major modes of monsoon phases. As monsoon wet phase refers to rainy season along with warm and moist winds blowing inland from the warm topical oceans, and the dry phase refers to the other half of the year when winds bring cool and dry air from the winter continents, both precipitation and winds of 12-month climatology are analysed.

Figure 1 presents the spatial patterns of the first EOF modes of the annual cycle of precipitation (Figure 1(a)), 925 hPa zonal wind (Figure 1(b)) and meridional wind (Figure 1(c)) along with their corresponding time series (Figure 1(d)). The first modes, which account for 66, 77 and 78% of the total variances respectively, show a contrast between the Northern Hemisphere (NH) and the Southern Hemisphere (SH) and between the large land masses and the oceans. Their corresponding time series depict the annual cycles with peaks in boreal winter and minimums in boreal summer. Combining the spatial patterns and the time series, the first EOF modes reflect the effects of the earth's orbit around the sun and of the thermal characteristics of the earth's surface (ocean and continent) The solar radiation and the land–ocean distributions are the first two primary driving forces of the global monsoon (Zeng and Li, 2002). In this sense, the first modes of the annual variations of the precipitation and winds represent the global monsoon, by and large. Note that the same phase persists in the months of May, June, July, August and September (MJJAS) in annual cycle in respect of the three components (Figure 1(d)), and this period is considered as the boreal summer monsoon time. Similarly, the

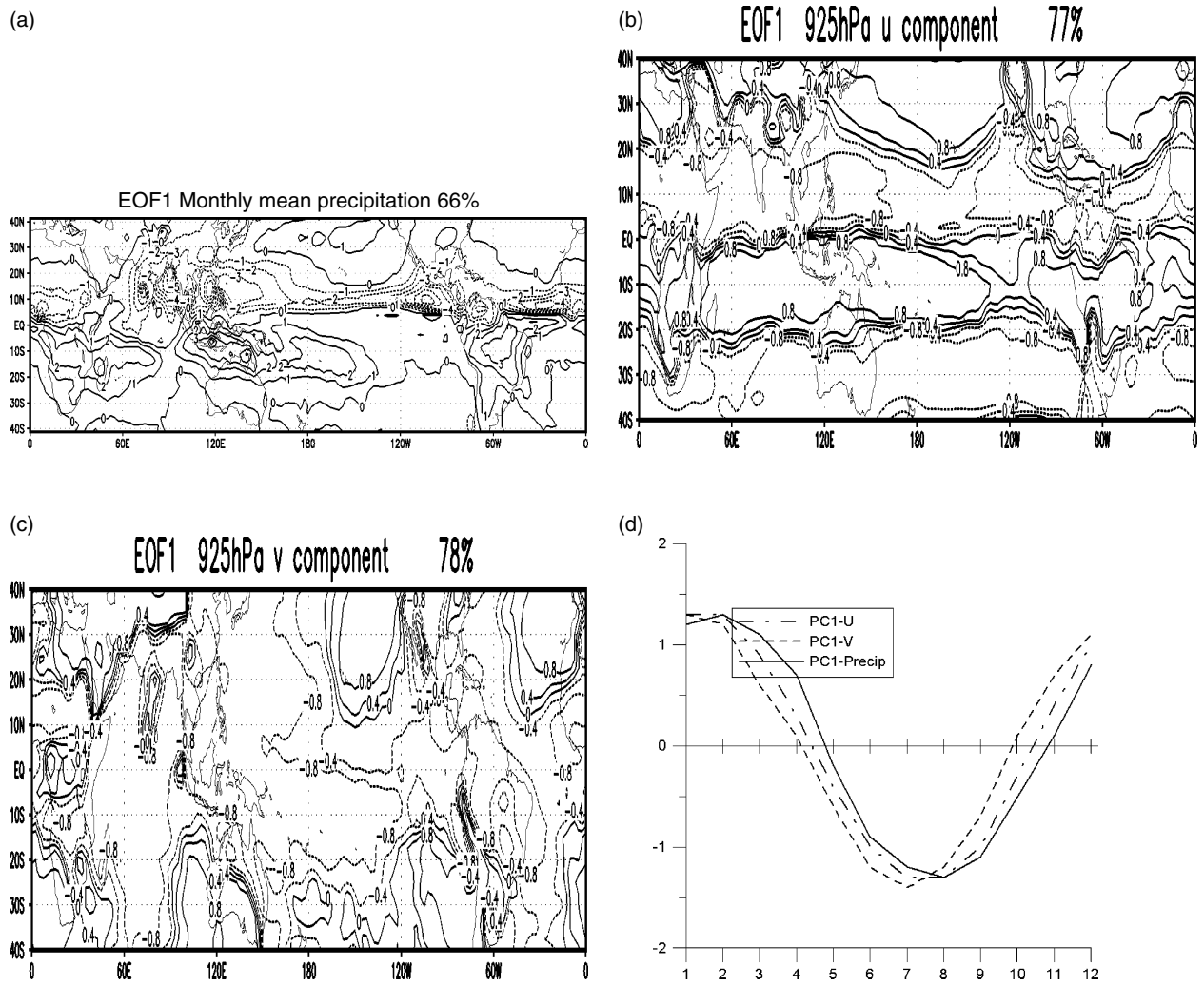

Figure 1. The spatial patterns of the first EOF modes: (a) the climatological monthly mean precipitation, (b) zonal wind, (c) meridional wind, and (d) their corresponding normalized time series. The precipitation is from the CMAP and the 925 hPa winds are from the ERA-40.

DOI: 10.1002/joc

months of November, December, January, February and March (NDJFM) is taken as the austral summer monsoon time.

3.2. Definition of the summer monsoon rainy season

It has been generally recognized that a typical monsoon rainy season implies significant concentration of yearly rainfall or a unimodal seasonal distribution, large precipitation rainfall annual range and an intense rainfall rate in the local summer (Wang, 1994; Wang and LinHo, 2002). Thus, three factors are considered here to describe quantitatively these characteristics: (1) the total amount of summer rainfall to measure the intensity of the rainy season (Figure 2(a)), (2) the annual range to measure the amplitude of annual rainfall variation (Figure 2(c)), and (3) the ratio of summer to yearly rainfall to measure the concentration of summer precipitation (Figure 2(d)). Figure 2(a) shows total summer (MJJAS for the NH, NDJFM for the SH) precipitation rate. The precipitation is below 3 mm/day in semi-arid and arid continents or over cold tongues. But this criterion (3 mm/day) seems unlikely to distinguish monsoon rainfall from non-monsoon rainfall in the Intertropical Convergence Zone (ITCZ), the South Pacific Convergence Zone (SPCZ) and the storm tracks in the mid-latitude oceanic areas where the rainy rate keeps over 3 mm/day nearly year round (Figure 2(a), (b)). Figure 2(c) shows the annual range. The largest annual range (the pentad maximum minus the pentad minimum) exceeding 14 mm/day appears mainly over the Arabian Sea, the Bay of Bengal, the SCS, the Philippine Sea, the Northeastern Tropical Pacific, the Northern Tropical Atlantic, the Southern Tropical Pacific and the Southern Tropical Indian Ocean. These regions seem to coincide with the maximum summer rainfall as shown in Figure 2(a). Figure 2(d) shows the percentage the summer rainfall accounts for of the total annual precipitation. The larger the ratio is, the wetter the summer. The large ratio exceeding 70% appears not only over the Indian monsoon region but also over the northeast of China, Korea, the tropical Africa, the northern Australia, the northeastern tropical Pacific and the southern tropical and subtropical America. Over the Philippine Sea, the ratio is relatively high (over 55%), while it is below 45% in ITCZ and storm tracks. Thus, the level of 55% provides a reasonable demarcation for the equatorial perennial precipitation and monsoon rainy seasons.

The distribution pattern of summer rainfall resembles basically that of the annual range (Figure 2(a), (c)), both of which can effectively distinguish the semi-arid continental regimes from the monsoon ones; and the ratio of summer to yearly rainfall can tell the differences of the equatorial perennial rain regimes and monsoon ones (Figure 2(d)). Therefore, we combine the two factors, summer rainfall rate and the ratio, to produce the domain of summer monsoon rainy season. The domain of the summer monsoon rainy season is defined as the region where the summer (MJJAS for the NH, NDJFM for the SH) rainfall must be equal to or above 3 mm/day and the ratio must be greater than 55%. The areas encircled by the solid lines in Figure 3 represent the summer monsoon rainy season domains delineated in this way.

3.3. Distributions of the global monsoon rainy season

There are six major monsoon rainy season domains at both sides of the equator: the ASM, the Indonesian and Australian summer monsoon (I-ASM), the North African summer monsoon (NAfSM), the South African summer monsoon (SAfSM), the North American summer monsoon (NAmSM) and the South American summer monsoon (SAmSM) (Figure 3). This climatological summer monsoon domains produced precisely by the objective criterion, have more delicate spatial structures, and,

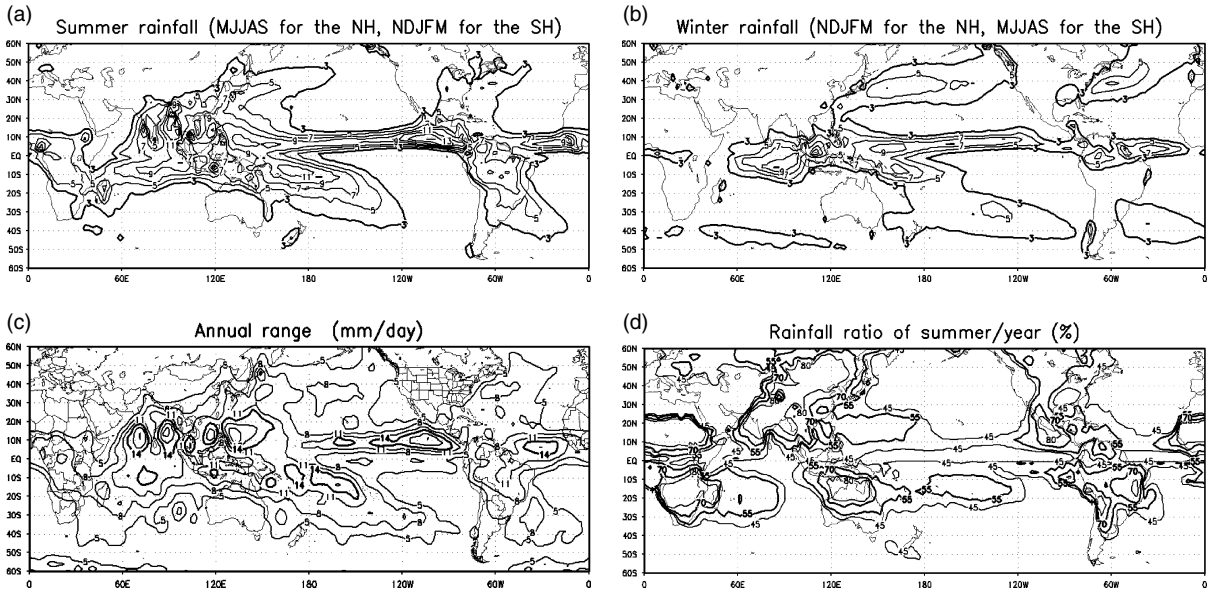

Figure 2. (a) Summer precipitation rate (mm/day), MJJAS for the NH and NDJFM for the SH, (b) winter precipitation rate (mm/day), NDJFM the NH and MJJAS for the SH, (c) annual range (pentad maximum minus pentad minimum, mm/day), (d) the ratio of summer to annual precipitation. The data are from the CMAP climatological monthly and pentad (5-day) mean.

DOI: 10.1002/joc

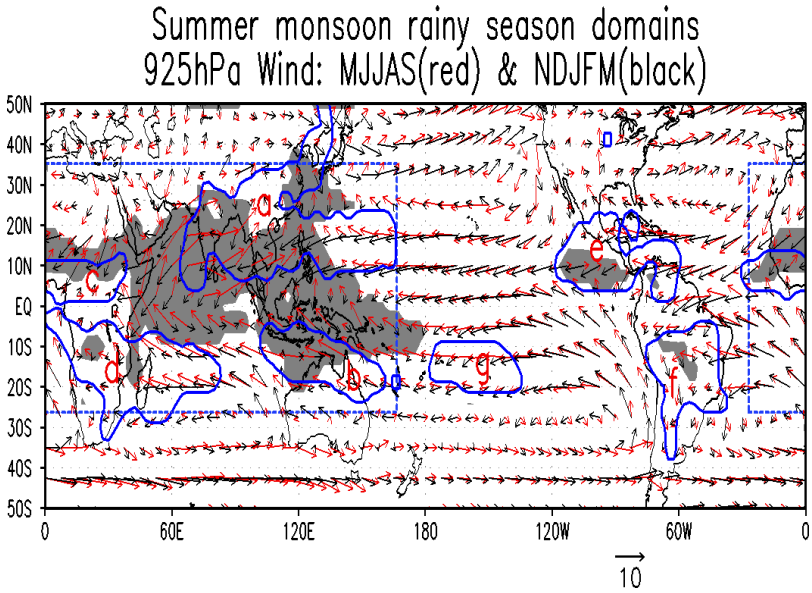

Figure 3. The summer monsoon rainy season domains (solid line) where the summer rainfall (MJJAS for the NH, NDJFM for the SH) is equal to or above 3 mm/day and the ratio of summer to annual rainfall is greater than 55% (a, ASM; b, I-ASM; c, NAfSM; d, SAfSM; e, NAmSM; f, SAmSM; g, CSPSM). The monsoon wind reversal domains (shaded areas) where the differences of summer and winter wind directions are greater than or equal to 90 degree, and the absolute values of wind speed are greater than or equal to 2 mm/s. The wind vectors (MJJAS for the NH and NDJFA for the SH). The monsoon regime from Ramage 1971 (dotted rectangles). The data used are CMAP precipitation and ERA-40 925 hPa wind. This figure is available in colour online at www.interscience.wiley.com/ijoc

thus, highlight the global summer monsoon rainy season domains, and are basically consistent with the classical tropical and subtropical monsoon domains proposed by previous studies using more complicated methods (e.g. Ramage, 1971; Wang, 1994; Wang and LinHo, 2002).

Figure 3 shows the following: (1) the summer monsoon rainy season domains are off the equatorial zone in both the hemispheres, thus excluding the equatorial perennial rainfall regions or bimodal variations, e.g. ITCZ in the Pacific and the Atlantic, (2) extratropical perennial or semi-perennial rainfall regions are excluded, e.g. the South Atlantic Convergence Zone (SACZ), major portion of the SPCZ, and storm tracks in the North Pacific and North Atlantic (Figure 2(a)–(b)), and (3) the present ASM domain stretches northward into the middle latitudes including primarily the Northeast China and Korea peninsula.

The immense Asian monsoon includes the East Asian summer monsoon (EASM) domain, the South China Sea summer monsoon (SCSSM) domain, the Indian summer monsoon (ISM) domain and the western North Pacific summer monsoon (WNPSM) domain (Figure 3). Note that the EASM domain covers the Korea peninsula and the Northeast China. Figure 4 supplies samples to convince the present resultant summer monsoon rainy season domains. The annual rainfall variation in the Northeast China (Figure 4(a)) is almost the duplication of the annual rainfall cycle in the West Africa (Figure 4(b)) that is a pronounced monsoon region. Earlier studies have discussed the existence of the mid-high latitude monsoon regions. The semi-permanent planetary waves in the mid-high latitudinal zones owing to the seasonal variations of thermal contrast of land and ocean (the secondary driving force) in phase with the incoming solar radiation (the first driving force) are favourable for the Asian–Australian monsoon to extend to the middle latitude regions (Zeng and Zhang, 1998; Zeng, 2000; Zeng and Li, 2002; Li and Zeng, 2005). Recent studies show that summer rainfall in the Northeast China is principally controlled by the East Asian summer monsoon. (Wang *et al*., 2006). The contribution of the land–ocean distribution can be easily found from comparison of Figure 4(a)–(c). The Northeast China, though around 43.75 °N latitude, experiences summer rainfall similar to Brazil (21.25 °S) and West Africa (13.75 °N). The present resultant domain excludes the southeastern China (28 °N, 115 °E), a place that experiences heavy spring precipitation due to the persistence of the southern China stationary front and is often in the power of the subtropical high in mid-summer.

The Indonesian–Australian monsoon covers a zonal region from the North Australia to the south of the Indonesian main islands, e.g. Sumatra and Kalimantan (Figure 3). This zonally oriented monsoon domain just crosses the average summer monsoon trough line given by Drosdowsky (1996) and is consistent with Ramage (1971) and Wang (1994). If we consider the monsoon to be contrasting with wet summer and dry winter, the equatorial Indonesia due to its annual permanent precipitation should be removed from the monsoon domain just as shown in Figure 3.

The NAfSM domain stretches zonally from 30 °W to 40 °E almost across the whole tropical continental section of North Africa including the tropical Atlantic (Figure 3). This area can be also referred to as the West Africa monsoon that is delineated from 18 °W to 25 °E by Sultan and Janicot (2000, 2003a), yet other studies examine

DOI: 10.1002/joc

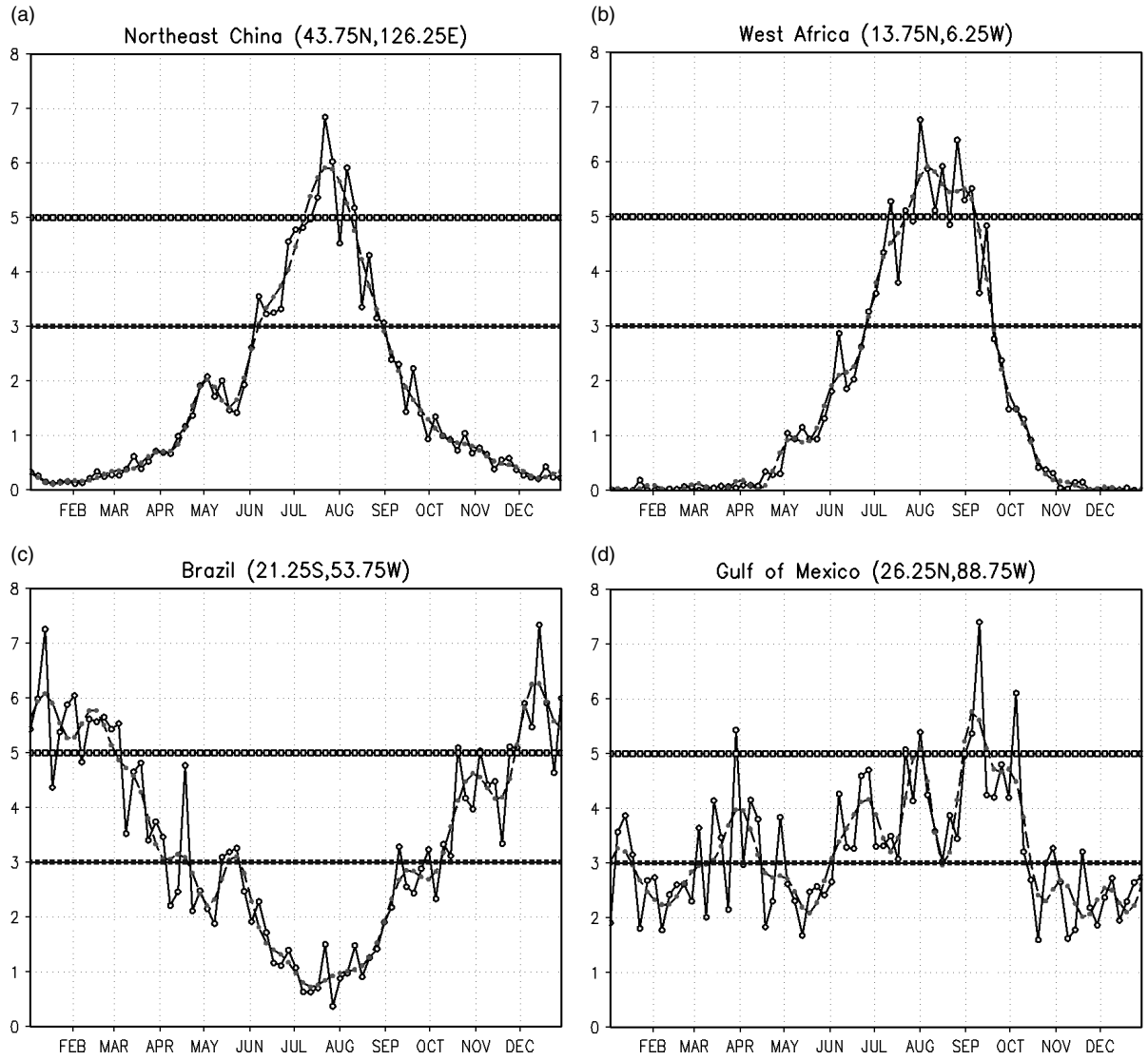

Figure 4. CPM precipitation rate (solid line with cycle mark) and RCPM precipitation rate (dashed line) at (a) 43.75 °N, 126.25 °E, (b) 13.75 °N, 6.25 °W, (c) 21.25 °S, 53.75 °W, (d) 26.25 °N, 88.75 °E. The two straight lines that mark the rainfall rate of 3 mm/day and 5 mm/day represent the rainy season domain and onset criteria respectively. The CPM climatology is derived from CMAP data for the period 1979–2004. Unit: mm/day.

the African monsoon from 10 °E to 40 °E (Trenberth *et al*., 2006) or from West Africa to the tropical Atlantic (Grodsky and Carton, 2001). Furthermore, the African rainy season derives from the back and forth migration of the ITCZ (Sultan and Janicot, 2000; Sultan and Janicot, 2003b), so this present resultant domain is reasonable. This monsoon region has been known as being the strongest expressions in zonal surface wind and cloud cover (Oubuih *et al*., 1999). The northern boundary of the NAfSM domain is nearly parallel to 15 °N latitude, the sub-Saharan region. The SAfSM domain (Figure 3) covers not only the tropical and subtropical continental South Africa but also the southwestern Indian Ocean that is often called the southwestern Indian Ocean summer monsoon (SWISM), and is consistent with Ramage (1971) and Wang (1994).

The NAmSM domain (Figure 3) is comprised of the eastern tropical North Pacific, the Central American isthmus; parts of the Gulf of Mexico and the Caribbean, and this domain is the main body of the Western Hemisphere Warm Pool (WHWP) marked by the obvious seasonal changes in tropospheric heat, moisture and stability resulting in contrasting wet and dry seasons (Wang and Enfield, 2001). The northern Gulf of Mexico and tropical Atlantic are excluded from the domain because of its mild seasonal contrast in precipitation (Figure 1(a)–(b), Figure 4(d)). Note that the NAmSM domain is not geographically consistent with the southwestern USA monsoon. The latter is primarily identified by means of synoptic data, located inland from Mexico into the southwestern United States, Arizona and New Mexico (Hawkins *et al*., 2002; Bordoni *et al*., 2004; Ellis *et al*., 2004), and cannot be revealed with this present global uniform criterion and the global climatological datasets.

Main portions of the SAmSM are in the interior region of Brazil (Figure 3), where (10–23 °S) about 75% of the annual rainfall occurs between 21 September and 21 March, and the winter is relatively dry

DOI: 10.1002/joc

(Rao *et al*., 1996). The La Plata Basin including Bolivia and North Argentina also has similar monsoonal variations in precipitation. The NAmSM and SAmSM domains, located from the 110 °W to 60 °W and from 80 °W to 40 °W respectively, are primarily in agreement with the American monsoon considered by Trenberth *et al*. (2006) and with the monsoon frame map given by Berbery *et al*. (2005) and Wang (1994).

Some regions are referred to as the oceanic summer monsoon (Murakami and Matsumoto, 1994; Wang and LinHo, 2002), for example, the WNPSM, the central South Pacific summer monsoon (CSPSM) and the SWISM. They are distinct from the continental summer monsoon domains by a weaker intensity of rainy season, a smaller rainfall ratio (Figure 1(a), (d)) and no complete reversals in horizontal winds (Figure 3). On the other hand, they have monsoonal rainfall pattern that is derived from the seasonal variations of the solar radiation. The warm water that favours the convection, though differing slightly in the criterion in different regions (Waliser *et al*., 1993), migrates back and forth following the sun. The precipitation maximum moves from tropics to subtropics apparently dragged by the poleward shift of the SST (sea surface temperature) maximum in the oceanic monsoon domains (Figure 5(a)–(c)). Similar situations can be found in the oceanic regions of the NAmSM (Xie, 2004).

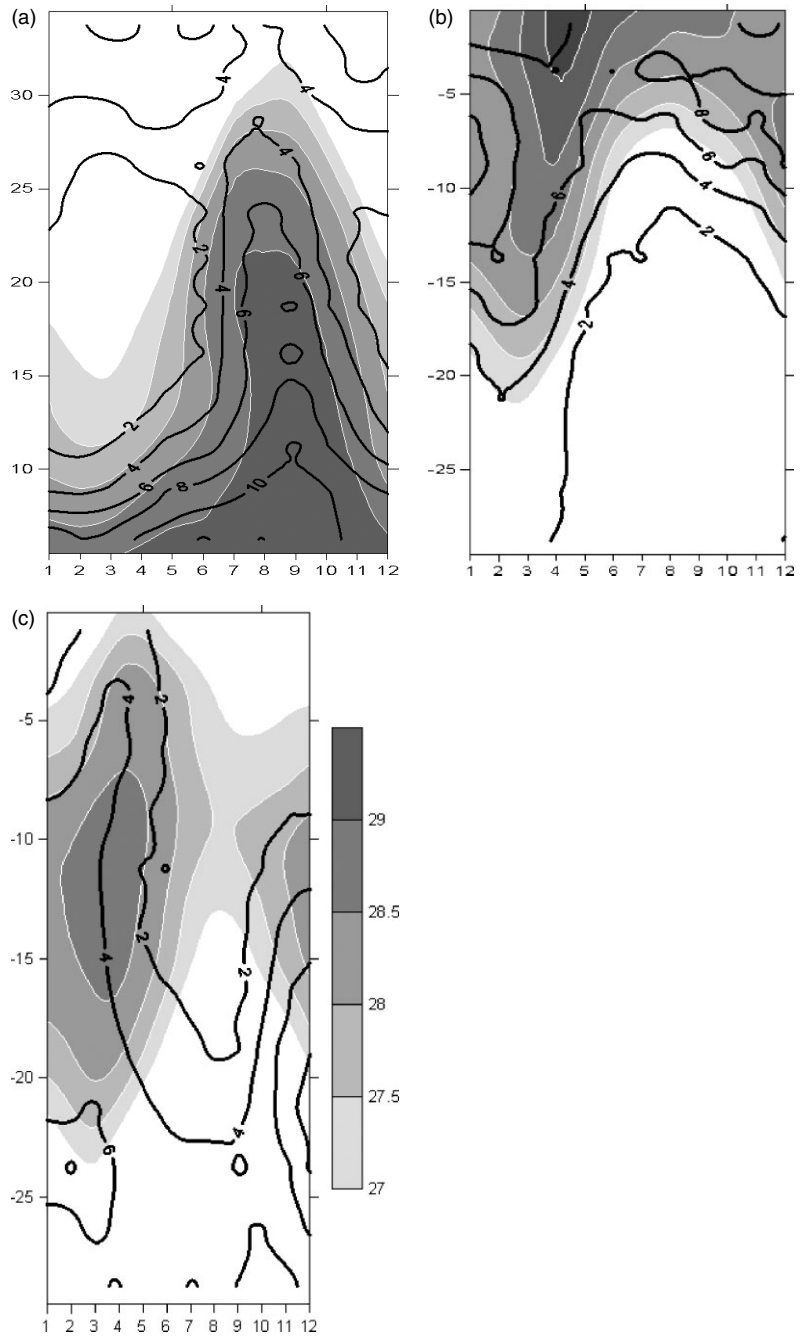

Figure 5. Latitude–time profile of SST and rainfall in oceanic summer monsoon domains. (a) WNPSM (156.5 °E), (b) SWISM (66.5 °E); (c) CSPSM (143.5 °W) Shaded: SST >27 °C, contour: precipitation rate (mm/day).

DOI: 10.1002/joc

Yet, the huge heat capacity and the dynamic mixing in oceans can hardly lead to reversals in SST gradient thus without any overturning in surface wind.

4. The onset, peak and withdrawal patterns

4.1. Definition of the onset, peak and withdrawal

Previous studies adopted some uniform criteria to define the local monsoon onset, for instance, a rainfall rate exceeding 6 mm/day (Lau and Yang, 1997) or climatological pentad mean (CPM) OLR below 230 W/m^2 (Murakami and Matsumoto, 1994). Such a uniform criterion is, perhaps, suitable for the tropical monsoon regions but is not applicable in a domain with a large latitudinal extent, because the intensity of the rainy season or convection varies considerably with latitude. A relative CPM rainfall rate defined by the difference between the pentad mean (R_i) and the January mean (R_{JAN}) precipitation rate could be able to solve the problem (Wang and LinHo, 2002). Yet the original CPM rainfall data might involve sub-monthly vibrations that are likely to reduce the stability of the procession of monsoon phase locking. In the present article, we use the RCPM CMAP data resulting from Fourier truncation with the sum of the first 12 harmonics to produce a uniform criterion, thus assuring a smoothed transition from onset, peak to withdrawal of monsoon. The relative RCPM rainfall rate is defined by:

$$RR_i = R_i - R_{\mathrm{JAN}}, i = 1, 2, \ldots, 73 \text{ (for the NH)}$$

$$RR_i = R_i - R_{\mathrm{JUL}}, i = 1, 2, \ldots, 73 \text{ (for the SH)}$$

in which R_i, R_{JAN} and R_{JUL} represent the RCPM precipitation, the CMAP climatological January mean and July mean respectively. The criterion, $RR_i \geq 5$ mm/day, has been proved to be able to reflect the onset date in the Asian monsoon region effectively (Wang and LinHo, 2002); therefore, this criterion is adopted in this study though the dataset is a reconstructed one and the scale is worldwide. Similarly, the transitional pentad in which the relative RCPM rainfall rate drops below 5 mm/day is defined as the withdrawal pentad. The peak phase is the pentad when the maximum RCPM rainfall rate occurs.

Note that a few spots of the domains may not qualify for the onset criterion ($RR_i \geq 5$ mm/day), and thus there would be no definite onset and withdrawal dates at these spots which are denoted by zero in Figures 6 and 8.

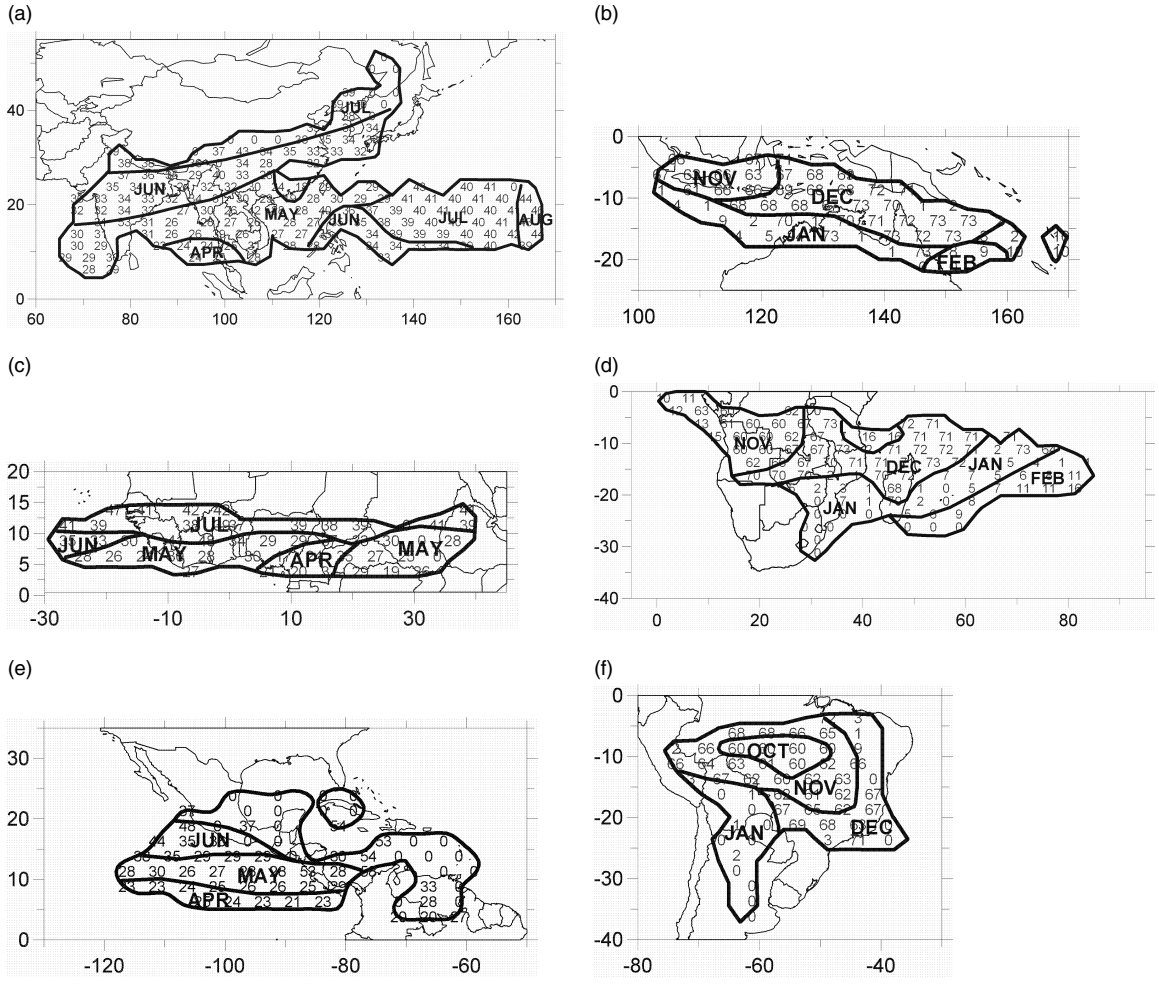

Figure 6. The dates of the onset phases of summer monsoon rainy season. Date/pentad. (a) the ASM, (b) the I-ASM, (c) the NAfSM, (d) the SAfSM, (e) the NAmSM, (f) the SAmSM.

DOI: 10.1002/joc

4.2. The onset patterns

4.2.1. The Asian and the Australian summer monsoon regions

Generally, in the immense Asian monsoon domains, the earliest onset of rainy season is found in late April (P24) over a limited area in the southeast Bay of Bengal (10 °N, 95 °E) (Figure 6(a)). The onset phase appears in the Indochina Peninsula in early May (P25–P27), a few days earlier than the date given by Tao and Chen (1987) but close to the date given by Tanaka (1992). In addition, the onset dates are a few days later than the date given by Matsumoto (1997) in which local *in situ* rainfall data have been utilized. These discrepancies show that smaller-scale local features may be omitted by CMAP or satellite data utilized by Tanaka (1992). The monsoon breaks out in the SCS in mid-May (P27–P28), agreeing with the mean onset date of P28 produced by different authors using alternative combinations of winds, OLR, gauged rainfall, θ_{se} and etc. (He *et al*., 2001). The onset phase progresses northward gradually in the ISM regions and eastward in a stepwise way in the WNPSM areas, which is well consistent with the results produced by Wang and LinHo (2002).

Over the Arabian Sea, the monsoon rain starting in late May (P28–P29) migrates northeastward rapidly reaching the southwest coast of the Indian subcontinent by P30–P31, and then moves northward to 20 °N by P32–P33, to the central India by P34–P35 and near 30 °N by P38. Another onset phase marches northwestward from the Bay of Bengal, approaching the east coast of India by P31. These two branches of onset phases (from the Arabian Sea and from the Bay of Bengal) reach India around P31, marking the beginning of the summer rainy season in the subcontinent. The pentads of monsoon onset are consistent with the onset dates defined by Tao and Chen (1987) and Tanaka (1992).

Over East Asia, the monsoon rainband moves to the lower reaches of Yangtze River and southern Japan by P32–P33, staring the Chinese mei-yu and Japanese baiu season. By late June (P34–P35), the monsoon rainband reaches South Korea, and the Korean Changma (Ho and Kang, 1988) starts. In northeast China and North Korea the summer rainy season begins in about P38–P39, which is in consistent with Tao and Chen (1987) and with other studies focusing on the North China rainy season, e.g. Zhao and Zhang (1996), and Wang *et al*. (2006). The synchronized onset of the Indian rainy season and the mei-yu/baiu forms a grand onset pattern in early June (P32–P33), which concurs with the early June reversal of the upper-tropospheric meridional temperature gradients in south Asia (Wang and LinHo, 2002).

The rainy season over the WNPSM domain shows an eastward stepwise propagating pattern. After taking place over the SCS-Philippine region in P27–P28, the onset phase appears to the southwestern Philippine Sea in about P33–P34 and then jumps northeastward causing the grand onset over the western North Pacific in P39–41, which is related to the phase-locked intraseasonal oscillation (ISO) over the region (Wu and Wang, 2001) and may involve physical processes of air–sea interaction (Wu, 2002).

The I-ASM rain starts in the tropical Java in early November (P61), and moves southeastward (Figure 6(b)). The onset occurs in the Timor Sea in P68, in the Coral Sea about P73, and finally reaches the southeast tip of the domain in early February (P8–P10). This eastward advance of monsoon onset phase is primarily related to the eastward propagation of the envelopes of the Madden Julian Oscillation (MJO) (McBride, 1987; Hendon and Liebmann, 1990; Wheeler and McBride, 2005). These climatological onset dates are compatible with what had been produced by Drosdowsky (1996) using 35-year observing data near Darwin.

4.2.2. The African summer monsoon regions

The onset phases in the NAfSM domain are obviously discontinuous (Figure 6(c)) reflecting its variable rainfall, which is the most significant climatic feature in the region driven by the continental position between the Earth's anti-cyclonic belts and its location astride the equator (NASA/Goddard Space Flight Center, Greenbelt, Maryland 20771 USA). The onset of rainy season occurs along the coast of the Gulf of Guinea around Cameroon in April from P20–P24, which corresponds to the first onset stage or the preonset of the West African summer monsoon (WASM) for the ITCZ is still located at 5 °N according to Sultan and Janicot (2003a). The first onset over the coastal region extends northward and the rainy belt jumps to 10–15 °N between 30 °W and 40 °E from P38 to P42, and this very narrow rainy belt is associated with the northward shift of the ITCZ from a quasi-stationary location at 5 °N to another quasi-stationary location at 10 °N and reflects the second onset stage of the WASM (Sultan and Janicot, 2003b). Another progression of rainy season seems zonal from Cameroon in P20–P24 across the coast of the Gulf of Guinea in May to the tropical Atlantic in June (P33–P35). This westward progression agrees with the westward propagating wave-like fluctuations revealed by Carlson (1969), Viltard *et al*. (1997), Diedhiou *et al*. (1998) and Grodsky and Carton (2001). In addition, the onset phases appear in the southern Sudan in May and in the northwestern part of Ethiopia in July, which is possibly linked with the ISM (Wang, 1994).

In South Africa, the rainfall is highly seasonal, with a pronounced dry season in the austral winter and an equally prominent wet season in the summer. The local rainy season starts progressively southeastward from the west coast of the equatorial South Africa in P60–P61 across the continent reaching the Mozambique Strait (20 °S, 35 °E) in P1–P7 next year (Figure 6(d)). Another eastward onset propagation occurs in the domain of the SWISM, starting over Madagascar in mid-December (P68–P70), arriving to 60 °E in P5–P7 and finally to about 80 °E in the tropical Indian Ocean in late February of the next year. The relatively earlier onset in Madagascar (P68–P70) compared to its surroundings as well as it eastward propagation further confirms the

DOI: 10.1002/joc

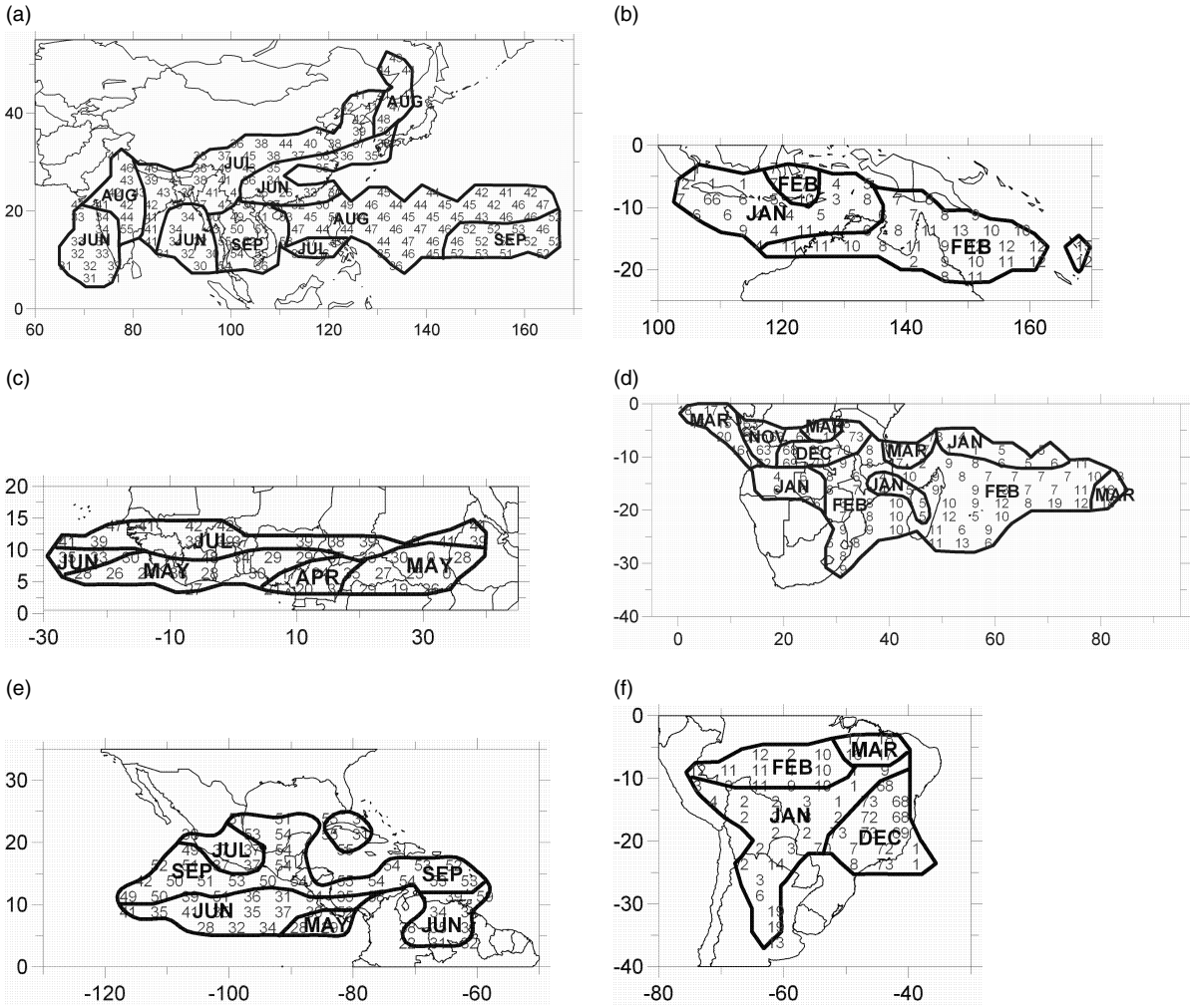

Figure 7. The date of the peak phases of summer monsoon rainy season. Others are as in Figure 6.

demarcation of the SWISM, an oceanic monsoon region that is a part of the Southwest Indian Ocean convergence zone (Cook, 2000) with seasonal contrast in precipitation (Figure 2).

4.2.3. The American summer monsoon regions

The onset phase propagates northward in the NAmSM region (Figure 6(e)). The rainy season starts in the equatorial northeastern Pacific in April, and then at around 10 °N in May, and at about 15 °N in June. This regulated northward migration is dragged by the warm water following the sun (Xie, 2004). The RCPM precipitation rate does not demonstrate the onset of the rainy season in the Caribbean Sea for the reason that we have explained in Section 4.1.

In the SAmSM, the rainy season occurs around the branches of the Amazon in Central Brazil in late October, and then expands to the surroundings in November (Figure 6(f)). The grand onset phases spread rapidly from P60 to P63 over the vast landmass of Brazil and stop to the east of the Andes. The combination of the heat source and the topography results in seasonal evolution of convection unique to this region (Charles *et al*., 2002). The northern part of Argentina and the southern part of Bolivia have summer rainy season but no obvious onset phases.

4.3. The peak pattern

The rainy season peaks first in June in four regions in the ASM domain: the central-eastern Arabian Sea, the Bay of Bengal, the southern SCS and the zone extending from the mid-lower reaches of the Yangtze River to the southern Kyushu, Japan, which is obviously associated with the subtropical front activities (mei-yu/baiu front) in East Asia (Figure 7(a)). The most splendid peak takes place in July from the northeastern India stretching northeastward to the lower reaches of the Yellow River, the Yellow Sea, the Korean Peninsula and the northeast of China. This grand synchronized peak from India to North China marks the height of the ISM and the EASM.

Generally, rainy season peaks later over the oceanic monsoon regions than over the adjacent continents because of the huge heat capacity of the oceans. August is the strongest period of the rainy season in the WNPSM domain (Figure 7(a)), and peak rainy season occurs in September around 10 °N, 160 °E that is in consonance with the enhanced tropical cyclonic activities near the

DOI: 10.1002/joc

date line during northern fall (Wang, 1994). Note that the rainy season in Indochina Peninsula peaks even later in September, which is possibly influenced by the activities of tropical cyclones and tropical lows that often take tracks westward in the tropical region once formed in the tropical Pacific in early autumn and by the westward-propagating disturbances that are originated from typhoons and take a more west-oriented track in the period (Fudeyasu *et al*., 2006). Actually, the rainy season over the Indochina Peninsula is of a bimodal pattern with a weaker peak in late May to early June caused by an intensification of the monsoon southwesterlies, a strong one in September related to tropical depressions and a distinct break in late June, which coincides with the seasonal march of the Asian monsoon in the region (Takahashi and Yasunari, 2006). Besides, the dates of the peak phase in the ASM domain are primarily in agreement with the results produced by Wang and LinHo (2002).

In the I-ASM, the peak of the rainy season, similar to the onset phase, progresses southeastward crossing the region from January to February. The height of the rain belt appears first in the Java Sea (5 °S, 110 °E) at the beginning of the year (P1), then comes close to the Timor Sea in P5 and final arrives to the Coral Sea (20 °S, 160 °E) in P12 (Figure 7(b)).

There are three major zonal peak belts in North Africa: the first one occurs in P31–P33 along the coast of the Gulf of Guinea near the equator, the second peak wave appears in P44–P48 in the northern section of the NAfSM domain, and the last one takes place in the central belt of the domain about 10 °N from 10 °W to 10 °E in P49–P50 (Figure 7(c)).

The peak phase propagates southeastward in a stepwise way (Figure 7(d)) in the South African continent. The peak appears first in the equatorial western continent (8 °S, 18 °E) in P63, at about 10 °S, 25 °E in P68–P70 and close to the east coast of the continent (20 °S, 35 °E) in early February (P7–P8). In the SWISM, the rainy season reaches its height in about P5 in Madagascar, and then spreads over the vast area of the tropical Indian Ocean (45–85 °E) with the last peak in P18–P19 at the east end of the SWISM domain.

The NAmSM is distinctive for the discontinuity in its peak patterns around the latitude of 10 °N between 60 and 120 °W (Figure 7(e)). The rainy season reaches its maximum in P35–P37 to the south of the latitude and in P50–P54 to the north of the latitude. This discontinuity reveals that there are other factors influencing the peak wet season besides the SST. The activities of tropical cyclones that often occur north of the 10 °N from late summer to early autumn in the East Pacific apparently play an important part in the formation of the peak rainfall, whereas hurricanes seldom take place within 10 °N, thus contributing to the discontinuity.

The SAmSM region is characterized by an equatorward retreat of the peak rainy season (Figure 7(f)). The peak rainy season appears in late December in the southeastern Brazil (25 °S, 45 °W), in early January in central South America (20 °S, 60 °W), in February over the Amazon Basin (10 °S, 60 °W) and by the end of March over the northeast of Brazil (7 °S, 45 °W).

4.4. The withdrawal pattern

There are three major equatorward withdrawal patterns in the ASM. The first one can be found in the WNPSM domain, where the rainy season retreats step by step slowly starting from 25 °N in August to 20 °N in September, 15 °N in October and finally 10 °N in November. The second one is in the ISM, where the rain belt starts to terminate in the Indian subcontinent in September, and then retreats to the northern Bay of Bengal in October and finally to the southern part of the Bay in November. The third equatorward withdrawal happens in the transitional region between the ISM and the EASM from the southeast side of the Himalayas to Indochina Peninsula lasting from July to December (Figure 8(a)). In contrast to the equatorward withdrawals, a northward retreat of the rainy season is found in East Asia, from the Taiwan Strait in P36, to the mouth of the Yangtse River in P39–P40, the lower reaches of the Yellow River in P43 and the northeast China in P45–P46. This seemingly odd feature is due to the fact that both the onset and withdrawal of the East Asian monsoon rainy season result from the northward migration of the monsoon front and the western Pacific subtropical high (Wang and LinHo, 2002).

By comparing the onset with withdrawal dates (Figures 6(a), 8(a)), it can be found that the rainy season generally lasts longer towards the equator. The rainy season in the EASM is about one month from the lower reaches of the Yangtse River valley to the Yellow River delta (30–38 °N, 120 °E) except in the vicinity of Korea (40 °N, 128 °E), where storm activities contribute to the prolonged rainy season. The wet summer lasts about 10–17 pentads over the Taiwan Strait. The longest rainy season is found from the Bay of Bengal to the SCS around 10 °N; which lasts about 40 pentads. The earliest retreats (P35–P36) are in the central-eastern Arabian Sea due in part to the rapid cooling of the western-central Arabian Sea after the outburst of the Somali jet. This early termination combining with the onset dates (P28–P29) leads to a shorter rainy season about 7 pentads though the area is located about 10 °N.

A large-scale withdrawal of rainy season occurs in March in the main body of the I-ASM domain (Figure 8(b)), which is close to the mean retreat date of 13 March given by Drosdowsky (1996). The earliest withdrawal is off the northwest coast of Australia (15 °S, 115 °E) in February leading to the shortest rainy season that lasts less than a month in the I-ASM domain, and retreat happens in April in the vicinity of Java causing the longest rainy season about 30 pentads in the domain.

The withdrawal dates vary widely from July (P38–P39) to December (P68–P72) in the tropical North Africa in spite of the rather narrow monsoon domain (Figure 8(c)). The first withdrawal occurs in a limited area over the coast of the Gulf of Guinea (8 °N, 8 °W) in P38–P39, and the final termination happens in the

DOI: 10.1002/joc

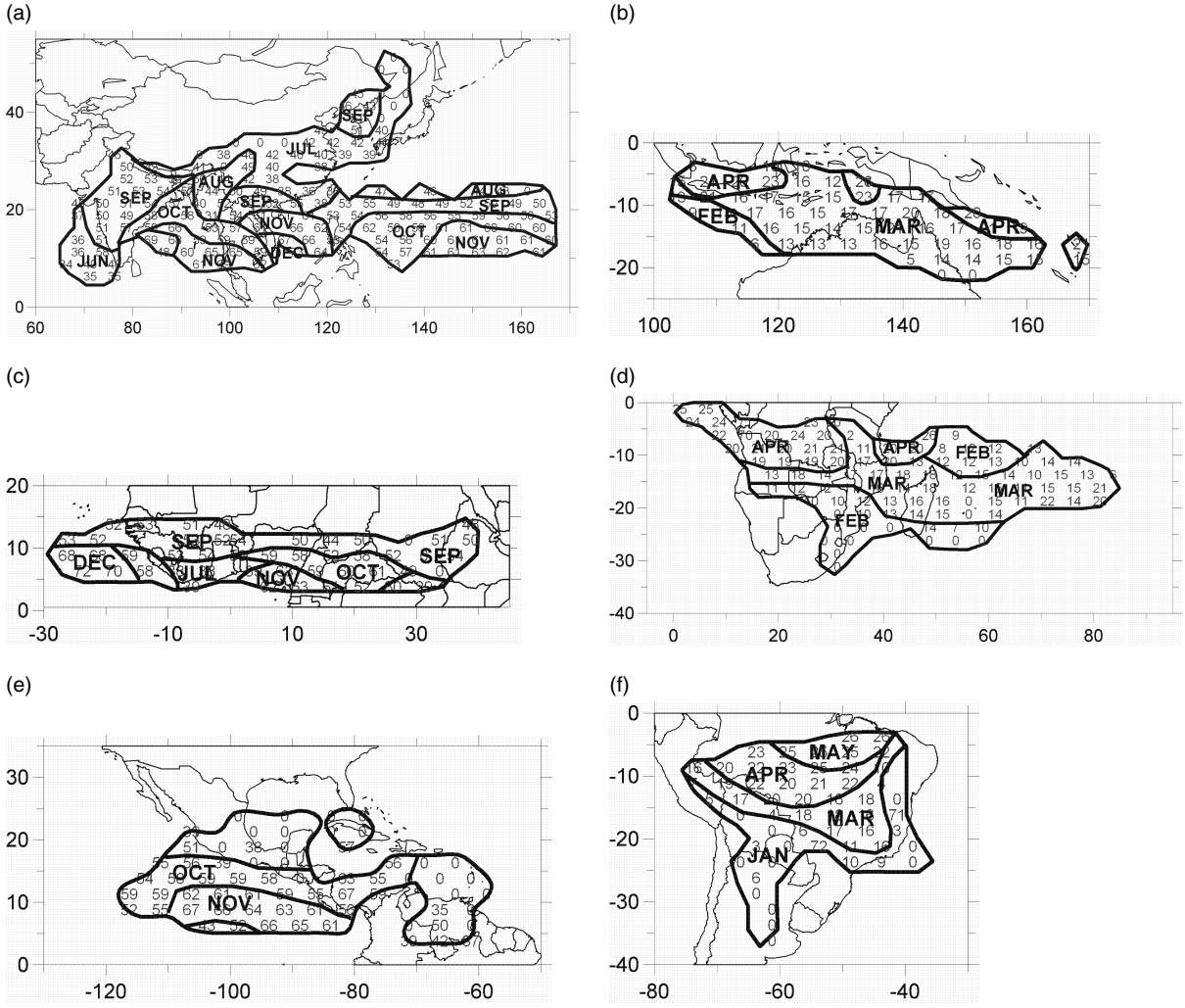

Figure 8. The date of the withdrawal phases of summer monsoon rainy season. Others are as in Figure 6.

tropical Atlantic (5–10 °N, 15–30 °W) in P68–P70 leading to about 40 pentads of the rainy season. The summer rainfall retreats from the narrow belt region of the Sudano-Sahelian in September (P52–P53) causing about 10 pentads of rainy season in this fragile environmental zone.

Figure 8(d) shows an equatorward withdrawal progression in the SAfSM, starting from the southeast coast of South Africa in P10–P12, across the continent in March and reaching to the northwest coast of the continent in P20–P24. Another overall retreat occurs in March (P13–P18) from the Mozambique Strait crossing Madagascar to the central Indian Ocean (Figure 8(d)). The major withdrawal in P13–P18 along with the onset in P5–P11 makes a rather short rainy season between 15 and 20 °S and 50 and 80 °E in the SWISM domain. This short rainy season in the tropical Indian Ocean reflects partially the sensitivity of the rain band to the sea surface temperature in the fringe area of warm water (Figure 5(b)). The length of the rainy season is about 34–37 pentads in the northwestern part of the tropical South African continent shaped by the poleward onset and equatorward withdrawal progressions in the SAfSM.

The withdrawals of rainy season in North and South America are apparently characterized by the regularly equatorward progression. In the NAmSM, the retreat starts in the northern part of the domain in P58–P59 and appears in the southern boundary of the domain in P65–P66 (Figure 8(e)). In the SAmSM, the rainy season withdraws from the southeast and southwest parts of the domain in January to the northeast end of the region in early May (P25–P26) (Figure 8(f)). The equatorward withdrawal propagations, along with the poleward onset pattern, lead to the longer rainy season near the equatorial zones in America (Figure 6(e), (f)).

The CSPSM is substantially related to the southeast portion of the SPCZ. The oceanic monsoon is weak because of the slight variations of the subtropical high in the SH. No reversals in winds are found in the region, yet the contrasting dry and wet season exists there because of the seasonal expansion and shrink of the warm SST driven by the sun (Figure 5(c)). The rainy season lasts shorter in the eastern part of the domain from December to February, and longer in the western sector from November to next March (Figures not shown).

DOI: 10.1002/joc

5. Discussions

5.1. Global monsoon regimes

So far, we have investigated the summer monsoon rainy season domains, onset, peak and withdrawal characteristics. Since monsoon is originally derived from the overturning in the surface prevailing winds, it is worthwhile making efforts to discuss monsoon in terms of winds. We use 925 hPa winds instead of surface winds as in Ramage's work (1971) to discuss seasonal wind reversals because the winds at 925 hPa that are about 700–800 m high above the sea level can represent the surface winds to a much large degree and can reduce the local topographic effect that can be noisy when we consider global monsoons. Other authors also use 925 hPa winds to discuss large-scale monsoon circulations. For example, Webster *et al*. (1998) use 925 hPa wind and OLR to describe the mean boreal summer and winter monsoon circulation in the eastern hemisphere, and Trenberth *et al*. select 925 hPa winds to illustrate and highlight meridional structures of the overturning monsoonal circulations because the flow at 925 hPa is more distinctive. Besides, winds in MJJAS and NDJFM are used to represent summer monsoon in the NH and the SH respectively for the similar reasons we have given in Section 3.1 and for in agreement with the precipitation, which is based on the results of EOF analysis. To the best of our knowledge, the coastal areas as well as the marginal seas of China, controlled by the notable East Asian monsoon, have northeasterlies (northwesterlies) in winter and southeasterlies (southwesterlies) in summer with the difference of about 90° (Figure 3). Therefore, it is sensible to take 90° as a criterion instead of 120° that is used by Ramage (1971). The definitions of the seasonal wind reversals are proposed in this article as follows: (1) the winds alter signs at least in one component (zonal or meridional component) from summer to winter, (2) the differences between the wind directions are equal to or greater than 90° and the differences between the wind speed exceed 2 m/s from summer to winter. The dark grey shaded areas in Figure 3 denote the monsoon regions demarcated by the above criteria using ERA-40 925 hPa wind data. The resultant areas revealed by Figure 3 primarily consist of the monsoon regime produced by Ramage (1971) in the tropical and subtropical Asian–Australian monsoon regions and African monsoon regions.

Combining rainfall and winds, we stratify the global monsoon into strong and weak categories. The typical strong monsoon regime is defined as the regions with pronounced seasonal reversals in winds and contrasting wet–dry seasons. From Figure 3 the main bodies of the ISM, the SCSSM, the EASM, the NAfSM and the I-ASM domains show apparent reversals in winds thus being strong monsoon regions. The weak monsoon regime is marked by the contrast between a wet summer and dry winter but with very weak or no wind reversals. These situations can be found in the SAfSM, the NAmSM, the SAmSM, the WNPSM and the CSPSM (Figure 3).

Besides the above monsoon domains, there are some areas with seasonal overturning in winds but not qualifying for the present criteria in terms of rainy season in the tropical Indian Ocean and Asian–Australian region. The most striking reversal is the Somali jet along with the cross-equatorial overturning (Figure 3) that is referred to as a 'lateral monsoon' (Webster *et al*., 1998), and has long been emphasized (Ramage, 1971). The low-level southwesterly jet gives rise to a major supply of moisture in support of the Asian monsoon and the formation of the jet is closely linked to the onset of the Indian monsoon (David and Peter, 2001; Fasullo and Webster, 2003). Furthermore, numerous studies have pointed out the close relationships in the Asian–Australian monsoon systems (e.g. Chen *et al*., 1991) and the linkage of the African–Western Arabian Sea monsoon to the enormous Asian–Australian monsoon (Trenberth *et al*., 2006). Thus, these tropical wind reversals are highly monsoonal.

Note that winds seemingly reverse in the subtropical North and South Pacific (Figure 3). These narrow belt regions, deriving substantially from the seasonal shift of the mid-latitude westerlies and comprising many transient baroclinic eddy activities, are not monsoonal if we take the monsoon as a steady circulation (Ramage, 1971). Furthermore, the annual circles of the precipitation, embedded in the storm tracks, are more or less Mediterranean pattern or semi-permanent pattern (Figure 2(a), (b)). Another seasonal overturning in winds exists in the mid-latitudes of East Europe–West Asia with southerlies in winter and northerlies in summer (Figure 3), which is opposite to the classical monsoon.

5.2. Contrast between results deriving from different datasets

Since the CMAP dataset is of multi-source including gauge observations and five different satellite estimates, the uncertainties and the model dependent limitations in the dataset are significantly reduced. Three major reanalysis precipitation datasets of ERA-40, JRA-25 and NCEP are used to produce the domains of summer monsoon rainy season to see how much they match the CMAP results.

Generally, the results produced by the three datasets are compatible with those by CMAP in the six major monsoon domains: the ASM, the I-ASM, the NAfSM, the SAfSM, the NAmSM and the SAmSM, yet some discrepancies still exist (Figure 9). The JRA-25 seems to slightly overestimate the precipitation in the subtropical regions leading to larger domains for the WNPSM and the I-ASM, and the biases are especially considerable in North America. The NCEP possibly underestimates the precipitation in the western North Pacific for it fails to capture large portions of the WNPSM, but on the other hand, it produces some monsoon domains in the mid-latitudes of Eurasia and North America by overestimating the precipitation. The ERA-40 seems to consist with the CMAP best in terms of monsoon delineation among

DOI: 10.1002/joc

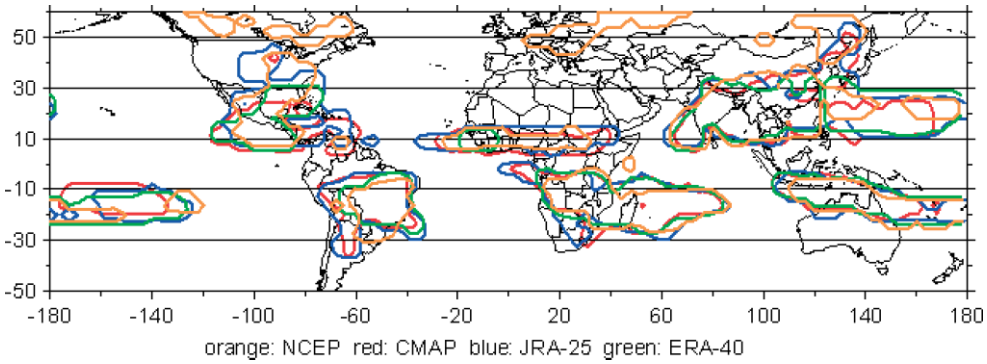

Figure 9. The summer monsoon rainy season domains derived from different datasets. Orange, NCEP; red, CMAP; blue, JRA-25; green, ERA-40.

the three datasets, yet some monsoon regions in North America, North Africa and East Asia are missed by it.

6. Conclusions

The original definition of monsoon is based on the annual reversal of surface winds. However, the meteorological significance and practical importance of rainfall makes it desirable to define summer monsoon rainy season domains. In this article, we have proposed a set of universal criteria for defining the domain, onset, peak and withdrawal of the global mean monsoon rainy season. On the basis of the EOF analysis of the climatological monthly mean rainfall and winds, the global summer monsoon period can be properly represented by the months from May to September for the NH and from November to March for the SH. The criteria of summer rainfall intensity ($\geq$3 mm/day) and the rainfall ratio (>55%) are combined to produce the six major domains of the summer monsoon rainy season in Asia, Australia, America and Africa. And an isolated monsoon domain is in the southern Pacific. The definitions and the corresponding criteria of summer monsoon rainy season are concise and objective, and the resultant domains coincide primarily with the regional summer monsoons defined by previous literatures. Wang and Ding (2006) also define the global monsoon precipitation domains according to annual precipitation range and summer rainfall ratio, which are equally concise and easy for application. Yet the present work focuses more on the rainy season characteristics, such as the onset, peak and withdrawal, which can reflect the spatial-temporal structure of the summer monsoon precipitation on a global perspective, and are essential for our understanding of monsoon dynamics and of significant importance for the improvement of our knowledge on the global climatology.

The RCPM precipitation and the corresponding criteria (relative RCPM rainfall rate $RR_i \geq 5$ mm/day) are used to determine the onset, peak and withdrawal phase of the summer monsoon rainy season. With this simple method, the global monsoon rainy season characteristics can be objectively and quantitatively described. Generally, rainy season starts in the tropics and then progresses poleward in the tropical and subtropical continental monsoon domains, while the propagation is rather zonal from west to east in the oceanic monsoon areas in both Hemispheres. The rainy season retreats equatorward causing longer wet summer in the tropics than that of the areas farther to the tropics. In addition, the rainy season lasts shorter close to the margins of the warm water where the cold water readily intrudes. The longer rainy season may last about 40 pentads, e.g. in the southern Bay of Bengal and SCS and northwestern tropical South Africa, while the shorter one may be only a month or so, e.g. in the central–eastern Arabian Sea and in East Asia. However, as one regulation has a hundred exceptions, some local rainy season patterns vary in others ways. For example, the poleward retreat pattern is found in the EASM, the westward onset progression is in the NAfSM and an apparently prolonged rainy season exits in Korean peninsula. The advance and retreat of rainy season are rather smoothly and regularly in regions like India, whereas the phases vary widely or discontinuously in some other regions like North Africa. The climatological dates of the onset, peak and withdrawal produced in the present study are definite, quantitative and primarily compatible with the other individuals who focus on local monsoon rainy season.

A comprehensive classification of global monsoon regimes is developed by taking both winds and precipitation into consideration. The global summer monsoon rainy season domains can be divided into two regimes: (1) the typical strong monsoon regime with contrasting wet–dry seasons and reversals in winds, including the domains of the ISM, the SCSSM, the EASM, the I-ASM and the NAfSM; (2) the weak monsoon regime with distinct wet summer and dry winter but no wind reversals as a whole, such as the WNPSM, the SAfSM, the CSPSM, the SAmSM and the NAmSM. Some areas in the tropics, though without pronounced rainy season, are highly monsoonal for the seasonal reversals in winds and cross-equatorial flows are very much linked with the typical strong monsoons, e.g. the vicinity of the Somali jet, the western Arabian Sea and the equatorial India Ocean. Whereas the areas that seemingly have seasonal overturning in winds are not monsoonal because the overturning is opposite to the classical monsoon reversal and the rainfall patterns are more or less Mediterranean not qualifying

DOI: 10.1002/joc

for the monsoon rainy season characteristics, e.g. the subtropical North and South Pacific.

A simple comparison is used to assess the performance of the three reanalysis datasets in respect of summer precipitation. The ERA-40, JRA-25 and NCEP show good capabilities in the identification of the major summer monsoon rainy season domains in the tropics and subtropics, but the NCEP and the JRA-25 are less realistic than the ERA-40 in the North American regions, the NCEP tends to overestimate the rainfall in the mid-latitudes and the ERA-40 seems to underestimate rainfall in Central America, North Africa and Northeast China. Since the current climate models have deficiencies in simulation of the summer monsoon, these resultant diagrams suggest that the continental and oceanic monsoons consist of integrated monsoon hydrological cycles, and the simple yet objective definitions of monsoon domain, onset, peak and withdrawal provide a useful validation tool for diagnosis of the (general circulation models) GCMs.

The global monsoon systems are very much enriched in their local structures influenced by the earth's revolution around the sun and by many other factors, such as the land–sea distribution, the interactions of the two Hemispheres and the topography. In addition, new observations, particularly, estimated from satellites could be able to supply more reliable data to modify this study results.

Acknowledgements

The authors deeply appreciate Xuxu and Wushu for their assistance in figure plotting. This research is supported by National Natural Science Foundation of China NSFC 40333030, Scientific and Technological Programs of Shandong Province, China, No. 2004GG2208111 and the 'Green Card' project of the Ocean University of China.

References

Adams DK, Comrie AC. 1997. The North American monsoon. *Bulletin of the American Meteorological Society* **78**: 2197–2213.

Anderson BT, Roads JO, Chen S, Juang HH. 2000. Regional simulation of the low-level monsoon winds over the Gulf of California and southwestern United States. *Journal of Geophysical Research* **105**: 17955–17969.

Berbery EH, Collini E, Silva V. 2005. *The American Monsoons and their Role in the Water Cycle*, http://www.uscliver.org/meeting_files/PanAm_0903/PanAm_monsoons_Berbery.pdf.

Bordoni S, Ciesielski PE, Johnson RH, McNoldy BD, Stevens B. 2004. The low-level circulation of the North American monsoon as revealed by QuikSCAT. *Geophysical Research Letters* **31**: L10109, Doi.10.1029/2004GL020009.

Carlson TN. 1969. Some remarks on African disturbances and their progress over the tropical Atlantic. *Monthly Weather Review* **97**: 716–726.

Charles J, Leila M, Carvalho V. 2002. Active and Break Phases in the South American monsoon system. *Journal of Climate* **15**: 905–914.

Chen LX, Zhu QG, Luo HB, He JH, Dong M, Feng ZQ. 1991. *The East Asian Monsoon*. Beijing Meteorological Press: Beijing; 362.

Cook KH. 2000. The South Indian convergence zone and interannual rainfall variability over Southern Africa. *Journal of Climate* **13**: 3789–3804.

David H, Peter MW. 2001. Somali Jet in the Arabian Sea, El Niño, and India rainfall. *Journal of Climate* **14**(3): 434–441.

Diedhiou A, Janicot S, Viltard A, Felice de P. 1998. Evidence of two regimes of easterly waves over West Africa and the tropical Atlantic. *Geophysical Research Letters* **25**: 2805–2808.

Drosdowsky W. 1996. Variability of the Australian summer monsoon at Darwin: 1957–1992. *Journal of Climate* **9**: 85–96.

Ellis AW, Saffell EM, Hawkins TW. 2004. A method for defining monsoon onset and demise in the Southwestern USA. *International Journal of Climatology* **24**: 247–265.

Fasullo J, Webster PJ. 2003. A hydrological definition of Indian monsoon onset and withdrawal. *Journal of Climate* **16**: 3200–3211.

Fudeyasu H, Lizuka S, Matsuura T. 2006. Seasonality of westward-propagating disturbances over Southeast and south Asia originated from typhoons. *Geophysical Research Letters* **33**: L10809, DOI:10.1029/2005GL025380.

Grodsky SA, Carton JA. 2001. Coupled land/atmosphere interactions in the west African monsoon. *Geophysical Research Letters* **28**(8): 1503–1506.

Hawkins TW, Ellis AW, Skindlov JA, Reigle D. 2002. Intra-annual analysis of the North American snow cover–monsoon teleconnection: seasonal forecasting utility. *Journal of Climate* **15**: 1743–1753.

He JH, Ding YH, Gao H, Xu HM (eds). 2001. *The Determination of the Onset of the South China Sea Summer Monsoon and the Indexes*. Meteorological Press: Beijing; 123 (in Chinese).

Hendon HH, Liebmann B. 1990. A composite study of onset of the Australian summer monsoon. *Journal of the Atmospheric Sciences* **47**: 2227–2240.

Ho CH, Kang IS. 1988. The variability of precipitation in Korea. *Journal of the Korean Meteorological Society* **24**: 1–15.

Kalnay E, Kanamitsu M, Kistler R, Collins W, Deaven D, Gandin L, Iredell M, Saha S, White G, Woollen J, Zhu Y, Leetmaa A, Reynolds B, Chelliah M, Ebisuzaki W, Higgins W, Janowiak J, Mo KC, Ropelewski C, Wang J, Jenne R, Joseph D. 1996. The NCEP/NCAR 40-year reanalysis project. *Bulletin of the American Meteorological Society* **77**: 437–471.

Lau KM, Yang S. 1997. Climatology and interannual variability of the southeast Asian summer monsoon. *Advances in Atlmospheric Sciences* **14**: 141–162.

Li JP, Zeng QC. 2005. A new monsoon index itsœ<u>a</u>interannual variability and relation with monsoon precipitation. *Climatic and Environmental Research* **10**(3): 351–365, (in Chinese).

Lin H, Wang B. 2002. The time-space structure of Asian summer monsoon-A fast annual cycle wiew. *Journal of Climate* **15**: 2001–2019.

Matsumoto J. 1997. Seasonal transition of summer rainy season over Indochina and adjacent monsoon region. *Advances in Atmospheric Sciences* **14**: 231–245.

McBride JL. 1987. The Australian summer monsoon. In *Monsoon Meteorology*, Chang CP, Krishnamurti TN (eds). Oxford University Press: New York; 203–231.

Murakami T, Matsumoto J. 1994. Summer monsoon over the Asian continent and western north Pacific. *Journal of the Meteorological Society of Japan* **72**: 719–745.

Oubuih J, de Felice P, Viltard A. 1999. Influence of the 6–9 day wave disturbances on temperature, vorticity and cloud cover over the tropical Atlantic during summer 1985. *Meteorology and Atmospheric Physics* **69**: 137–144.

Ramage CS. 1971. *Monsoon Meteorology*. Academic Press: New York; 296.

Rao YP. 1976. *Southwest Monsoon*, *Synoptic Meteorology, Meteorological Monography, No. 1*. Indian Meteorology Department: New Delhi; 367.

Rao VB, Cavalcanti IFA, Hada K. 1996. Annual variation of rainfall over Brazil and water vapour characteristics over South America. *Journal of Geophysical Research* **101**(D21): 26–539–26–551.

Sakamoto K, Tsutsui J, Koide H, Sakamoto M, Kobayashi S, Hatsushika H, Matsumoto T, Yamazaki N, Kamahori H, Takahashi K, Kadokura S, Wada K, Kato K, Oyama R, Ose T, Mannoji N, Taira R. 2007. The JRA-25 reanalysis. *Journal of the Meteorological Society of Japan* **85**(3): 369–432.

Simmons AJ, Gibson JK. 2000. The ERA-40 Project Plan. ERA-40 Proj. Rep. Ser. 1. European Center for Medium-Range Weather Forecasting: Reading; 63.

Sultan B, Janicot S. 2000. Abrupt shift of the ITCZ over West Africa. *Geophysical Research Letters* **27**: 3353–3356.

Sultan B, Janicot S. 2003a. The West African monsoon dynamics. Part I: documentation of intraseasonal variability. *Journal of Climate* **16**: 3389–3406.

Sultan B, Janicot S. 2003b. The West African monsoon dynamics. Part II: The "Preonset" and "Onset" of the summer monsoon. *Journal of Climate* **16**: 3407–3427.

Takahashi HG, Yasunari T. 2006. A climatological monsoon break in rainfall over Indochina–a singularity in the seasonal march of the Asian summer monsoon. *Journal of Climate* **19**: 1545–1556.

Tanaka MN. 1992. Interaseasonal oscillation and the onset and retreat dates of the summer monsoon over the east, southeast and western north Pacific region using GMS high cloud amount data. *Journal of the Meteorological Society of Japan* **70**: 613–629.

Tao SY, Chen L. 1987. *A Review of Recent Research on the East Asian Summer Monsoon in China. Monsoon Meteorology*, Chang C-P, Krishnamurti TN (eds). Oxford University Press: Oxford; 60–92.

Trenberth KE, Stepaniak DP, Caron JM. 2000. The global monsoon as seen through the divergent atmospheric circulation. *Journal of Climate* **13**: 3969–3993.

Trenberth KE, Hurrell JW, Stepaniak DP. 2006. *The Asian Monsoon: Global Perspectives. The Asian Monsoon*, Wang B (ed.). Springer/Praxis Publishing: New York; 787 pp.

Viltard A, de Felice P, Oubuin J. 1997. Comparison of the African and 6–9 day wave-like disturbance pattern over West-Africa and the tropical Atlantic during summer 1985. *Meteorology and Atmospheric Physics* **62**: 91–99.

Waliser DE, Graham NE, Gautier C. 1993. Comparison of the highly reflective cloud and outgoing longwave radiation datasets for use in estimating tropical deep convection. *Journal of Climate* **6**: 331–353.

Wang B. 1994. Climatic regimes of tropical convection and rainfall. *Journal of Climate* **7**: 1109–1118.

Wang B, Xu X. 1997. Northern hemispheric summer monsoon singularities and climatological intraseasonal oscillation. *Journal of Climate* **10**: 1071–1085.

Wang CZ, Enfield DB. 2001. The tropical Western Hemisphere warm pool. *Geophysical Research Letters* **28**: 1635–1638.

Wang B, Lin Ho. 2002. Rainy season of the Asian-pacific summer monsoon. *Journal of Climate* **15**: 386–398.

Wang B, Ding Q. 2006. Changes in global monsoon precipitation over the past 56 year. *Geophysical Research Letters* **33**: L06711, DOI:10.1029/2005GL025347.

Wang B, Wu R, Li T. 2003. Atmosphere–Warm ocean interaction and its impacts on Asian–Australian monsoon variation. *Journal of Climate* **16**: 1195–1211.

Wang XZ, Sun ZB, Tan YK, Hu BH. 2006. Demarcation and features of northeast China rainy season. *Journal of Nanjing Institute of Meteorology* **29**(2): 203–208 (in Chinese).

Webster PJ, Magana VO, Palmer TN, Shukla J, Tomas1 RA, Yanai M, Yasunari T. 1998. Monsoons: processes, predictability, and the prospects for prediction. *Journal of Geophysical Research* **103**(C7): 14 451–14 510.

Wheeler MC, McBride JL. 2005. *Australian-Indonesian Monsoon: Intraseasonal Variability in the Atmosphere-Ocean Climate System*, Lau WKM, Waliser DE (eds). Praxis Publishing: Springer Berlin Heidelberg; 125–173.

Wu R. 2002. Processes for the Northeastward advance of the summer monsoon over the western north pacific. *Journal of the Meteorological Society of Japan* **80**: 67–83.

Wu R, Wang B. 2001. Multi-stage onset of the summer monsoon over the western North Pacific. *Climate Dynamics* **17**: 277–289.

Xie SP. 2004. The shape of continents, air-sea interaction, and the rising branch of the Hadley circulation. In *The Hadley Circulation: Past, Present and Future*, Diaz HF, Bradley RS (eds). Kluwer Academic Publishers: Dordrecht; 121–152.

Xie P, Arkin PA. 1997. Global precipitation: A 17-year monthly analysis based on gauge observation, satellite estimates and numerical model outputs. *Bulletin of the American Meteorological Society* **78**: 2539–2558.

Zeng QC. 2000. *The Global Monsoon systemœrProceedings of the Second International Symposium on Asia Monsoon Systern (ISAM2) œªChejuœªKoreaœªMeteorological Research Institute (METRI) and Korea Meteorologieal Administration (KMA)*œª 23–27.

Zeng QC, Zhang BL. 1998. On the seasonal variation of atmospheric general circulation and the monsoon. *Sientia Atmospherica Sinica* **22**(6): 805–813, (in Chinese).

Zeng QC, Li JP. 2002. Interactions between the Northern and Southern hemispheric atmospheres and the essence of monsoon. *Chinese Journal of Atmospheric Scienses* **26**(4): 433–448.

Zhao HG, Zhang XG. 1996. The Relationship between the Summer Rain Belt in China and the East Asia Monsoon. *Meterological Monthly* **22**: 8–12, (in Chinese).

DOI: 10.1002/joc